Squeezed vacuum states in a nonlinear medium modulated by periodic kicking

Christopher C. Gerry
Department of Physics, St. Bonaventure University, St. Bonaventure, New York 14778

Rainer Grobe
Department of Physics and Astronomy, University of Rochester, Rochester, New York 14627

Edward R. Vrscay
Department of Applied Mathematics, University of Waterloo, Waterloo, Ontario, Canada N2L 3G1
(Received 2 July 1990)

In this paper we study the dynamics of a nonlinear quantum-optical system subjected to a periodic modulation in the form of kicks. The system consists of a nonabsorbing anharmonic medium related to optical bistability, a degenerate parametric amplifier with a classical pump field that is modulated by a periodic sequence of kicks, and the initial state is taken to be a squeezed vacuum state. Using the related SU(1,1) coherent states (which are squeezed vacuum states), we study and compare the quantum and classical dynamics of the system. The "classical" motion in this case means the motion projected onto the phase space defined by the parameter labeling the generalized coherent states. For certain values of the coupling constants, we obtain both regular and chaotic motion in the classical phase space. In the quantum dynamics of the system, the manifestation of the classical chaos turns out to be rather weak, at least in the regime numerically accessible to us. We study the time evolution of the initial-state population probability, the average photon number in the field, and the squeezing of the field. We also briefly discuss the level statistics of the evolution operator.

I. INTRODUCTION

The study of quantum systems whose classical counterpart exhibits chaotic behavior has been of great interest in recent years.[1] A particularly interesting class of problems is concerned with systems driven with a periodic sequence of nonlinear kicks. Zaslavsky,[2] for example, has studied a nonlinear, anharmonic oscillator undergoing a series of periodic kicks and has projected the resulting solutions of the Heisenberg equations onto the quantum phase space associated with the usual harmonic oscillator coherent states. Such states have also been used as an alternative to the pure momentum eigenstates in the study of the quantum dynamics of the kicked rotator.[3,4] On the other hand, quantum and classical chaos for a top kicked by a nonlinear interaction has been studied with the aid of coherent states associated with the group SU(2).[5] In this case the natural phase space is just the Bloch sphere (or a projection of the Bloch sphere onto a plane). The quantum dynamics takes place in a finite dimensional Hilbert space due to the fact that the squared angular momentum is a constant of the motion. A distinction between regular and irregular behavior could be made for times exceeding the quantum-mechanical quasiperiod at which the classical description becomes inappropriate.

Other kinds of quantum states have also been studied in quantum chaotic systems. Of particular interest in the area of quantum optics is the so-called squeezed state, well known to have no classical analog in the sense that it cannot be represented by a true probability distribution in phase space (i.e., the P function being nonpositive definite).[6] Recently, Życzkowski[7] has studied the time evolution of squeezed states in the kicked rotator model. He has found that squeezing influences the shape of quantum revivals obtained in the regime of classically regular motion but does not facilitate the diffusion in the angular momentum in the regime of classical chaos. Furthermore it was noted that the speed of unlimited energy growth, which occurs in the case of quantum resonance, depends significantly on the squeezing parameter. It must be mentioned, however, that squeezed states have so far been produced only in quantum-optical experiments.[8] It is difficult to see how squeezed states in a quantum kicked rotator could be experimentally realized.

In this paper the time evolution of squeezed states is studied for a case which we believe to be more realistic than the one described in Ref. 7. We consider a single-mode squeezed state, specifically a squeezed vacuum state, in a nonlinear medium which consists of a nonabsorbing anharmonic oscillator and a degenerate parametric amplifier with a classical pump field. Such a system has been shown to be related to optical bistability[9] and has previously been shown to produce states of enhanced squeezing from ordinary coherent light.[10,11] The evolution of squeezed vacuum states has also been studied for such a system.[12] In the present study, however, the pump field is taken to be modulated by an infinite sequence of δ-function kicks.

To analyze the model, we find it very convenient to make use of the fact that the problem has a natural rela-

tionship to the dynamical group SU(1,1). It has been shown previously[13–15] that the squeezed vacuum state is nothing more than a generalized coherent state associated with SU(1,1) as given by the Perelomov definition.[16] Coherent states (CS) associated with SU(1,1) have been studied in great detail[17,18] and have previously been used in the study in the interaction of the squeezed vacuum with two-level atoms[19] and nonlinear media.[15,20] Like the usual harmonic oscillator (ordinary) CS and the SU(2) CS, the SU(1,1) CS's have an associated phase space which, in this case, takes the form of the Lobachevski plane. It is therefore possible to project the "classical" motion of the SU(1,1) CS into this phase space for any Hamiltonian system that can be written in terms of the generators of the group. Of course, only in the case when the Hamiltonian is linear in the generators do the quantum and classical motions agree in the sense that the coherence of the initial state is preserved.[14] In the model to be discussed in this paper, the Hamiltonian may be expressed in terms of the boson realization of the SU(1,1) Lie algebra which has been used in previous studies.[13–15,19,20] Since our Hamiltonian will be quadratic in the SU(1,1) generators, the problem we study may be considered as the "noncompact" analog of the kicked top problem studied in Ref. 5. The principal difference in our case, however, is that the Hilbert space is necessarily infinite dimensional. Unlike for SU(2), this has the potential for introducing truncation errors in the quantum analyses. We should also mention here that previously a quasiperiodically kicked *linear* SU(1,1) system was studied:[21] the quantum and classical maps were shown to be essentially Möbius transformations in the representation of the Lobachevski plane for which the motion is confined to the interior of the unit circle in the complex plane. Even though there is no classical chaos, some of the supposed signals of quantum chaos, such as decay of the autocorrelation function and broadband power spectrum, do appear. This was previously shown for the case of the linear, quasiperiodically driven two-level system as well.[22,23]

This paper is organized as follows. In Sec. II we present the model and analyze the "classical" dynamics in terms of the evolution of an initial SU(1,1) CS which we take to be a squeezed vacuum state. The classical maps are also unimodular, time-dependent Möbius transformations which map the phase space onto itself one to one. When the anharmonic term is removed, they reduce to a single map. We also obtain a Heisenberg-type representation of the classical motion in terms of the elements of the Lie algebra which are allowed to commute in the "classical" limit in a manner defined below. In Sec. III are presented the numerical results of the classical map. As well, the quantum evolution is studied. In Sec. IV the paper is concluded with a brief summary.

II. MODEL

In this section we discuss the Hamiltonian of the model, cast it in terms of the SU(1,1) generators, and derive the quantum and classical maps for the associated SU(1,1) CS which we take to be a squeezed vacuum state. We shall not give any detailed review of the SU(1,1) CS formalism but will introduce the necessary concepts as needed in the discussion.

The Hamiltonian of our model system is

$$H=\hbar\omega_0(a^\dagger a+\tfrac{1}{2})+\tfrac{1}{2}\hbar\lambda(a^\dagger)^2a^2 +\tfrac{1}{2}\hbar\gamma[a^2e^{2i\omega_0 t}+(a^\dagger)^2e^{-2i\omega_0 t}]\delta_p(t) . \tag{2.1}$$

The first term represents the free field of frequency ω_0. The second term is an anharmonic term which gives rise to optical bistability, where λ is related to the third-order susceptibility of the medium. Finally, the last term essentially represents a degenerate parametric amplifier where the pump field has frequency $2\omega_0$ and is treated classically. The parameter γ contains a second-order susceptibility and the amplitude of the pump field. The pump field, however, is being modulated by a periodic string of δ functions $\delta_p(t)$ where

$$\delta_p(t)=\sum_{n=0}^{\infty}\delta(t-nT) , \tag{2.2}$$

and T is sufficiently large so that $\omega_0\gg 2\pi/T$. We now cast the above Hamiltonian into SU(1,1) form by using the following oscillator realization of the su(1,1) Lie algebra:

$$K_0=\tfrac{1}{4}(a^\dagger a+aa^\dagger),\quad K_+=\tfrac{1}{2}(a^\dagger)^2,\quad K_-=\tfrac{1}{2}a^2 , \tag{2.3}$$

satisfying the commutation relations

$$[K_0,K_\pm]=\pm K_\pm,\quad [K_+,K_-]=-2K_0 . \tag{2.4}$$

For later use, we introduce an alternate form of the Lie algebra. Defining $K_\pm\equiv K_1\pm iK_2$, we have

$$[K_1,K_2]=-iK_0,\quad [K_2,K_0]=iK_1,\quad [K_0,K_1]=iK_2 . \tag{2.5}$$

The Hamiltonian of Eq. (2.1) becomes

$$H(t)=2\hbar\omega_0K_0+2\hbar\lambda K_+K_- +\hbar\gamma(K_+e^{-2i\omega_0 t}+K_-e^{2i\omega_0 t})\delta_p(t) . \tag{2.6}$$

In order to remove the rapid $2\omega_0$ oscillations from the Hamiltonian, we transform to the interaction picture. With $H_0=2\omega_0K_0$, the Hamiltonian in the interaction picture is

$$H_I(t)=2\lambda K_+K_-+2\gamma K_1\delta_p(t) \tag{2.7}$$

where we have used the fact that $[K_0,K_+K_-]=0$ and the relations

$$e^{iH_0t/\hbar}K_\pm e^{-iH_0t/\hbar}=K_\pm e^{\pm 2i\omega_0 t} . \tag{2.8}$$

Now the evolution operator over a pulse may be written as

$$U_p=e^{-2i\gamma K_1} , \tag{2.9}$$

and the "free" (nonpulsed) evolution operator between the pulses is given by

$$U_f = e^{-2i\lambda T K_+ K_-} , \tag{2.10}$$

where T is the time between pulses. Thus through one pulse up to just before the next one, the evolution operator is given by

$$U = U_f U_p = e^{-2i\lambda T K_+ K_-} e^{-2i\gamma K_1} . \tag{2.11}$$

Before we go on to study the classical and quantum evolutions for this system, it is worthwhile to point out that there is a constant of the motion, namely, the Casimir operator of SU(1,1). We also take an opportunity to briefly review the relevant irreducible representations of the group and introduce the associated coherent states.

$$C = K_0^2 - K_1^2 - K_2^2 = K_0^2 - \tfrac{1}{2}(K_+ K_- + K_- K_+) . \tag{2.12}$$

Clearly

$$[H, C] = [U, C] = 0 . \tag{2.13}$$

Now we introduce the unitary representations of SU(1,1) known as the positive discrete series $\mathcal{D}^+(k)$ where k is a number determined from the eigenvalues of C which are traditionally written as $k(k-1)$. k is known as the Bargmann index and for $\mathcal{D}^+(k)$, $k > 0$. In these representations the operator K_0, which generates a compact subgroup, is diagonal. Denoting the basis states as $\{|m,k\rangle\}$ we have

$$K_0 |m,k\rangle = (m+K)|m,k\rangle, \quad m = 0,1,2,\ldots . \tag{2.14}$$

and

$$C|m,k\rangle = k(k-1)|m,k\rangle . \tag{2.15}$$

For the realization of the algebra of Eq. (2.3), it follows that $C = -\frac{3}{16}$ or that $k = \frac{1}{4}, \frac{3}{4}$. The relation between the SU(1,1) basis $|m,k\rangle$ and the usual Fock space number states $|n\rangle$ is quite straightforward. From K_0 in Eq. (2.3) and $[a, a^\dagger] = 1$, the number operator is given by

$$N = a^\dagger a = 2K_0 - \tfrac{1}{2} . \tag{2.16}$$

Thus $n = 2m + 2k - \frac{1}{2}$. For $k = \frac{1}{4}$, $n = 2m$ (n even), and for $k = \frac{3}{4}$, $n = 2m + 1$ (n odd). Thus the Hilbert space of the oscillator states is divided into two parts: $k = \frac{1}{4}$, even parity and $k = \frac{3}{4}$, odd parity. The fact that C and H commute is merely a statement of the fact that H preserves the parity (k) of the initial state.

The SU(1,1) coherent states are constructed in the usual way by the Perelomov definition.[16] They are given by

$$|\xi,k\rangle = S(z)|0,k\rangle = (1-|\xi|^2)^k \sum_{m=0}^{\infty} \left[\frac{\Gamma(m+2k)}{m!\Gamma(2k)} \right]^{1/2} \xi^m |m,k\rangle \tag{2.17}$$

where

$$S(z) = \exp(zK_+ - z^* K_-) \tag{2.18}$$

is the squeezing operator, $z = -\theta/2 e^{-i\phi}$, and $\xi = -\tanh(\theta/2) e^{i\phi}$. The angles θ and ϕ parametrize the SU(1,1) group manifold and have ranges $0 \le \theta < \infty$, $0 \le \phi \le 2\pi$. The complex number ξ, for which $0 \le |\xi| < 1$, parametrizes the phase space as do the angles θ and ϕ. The latter parametrize a hyperboloid which is the analog of the Bloch sphere of SU(2). The parameter ξ is essentially a projection of the hyperbolic surface onto the interior of the unit circle on the complex plane.[24] We shall use the parameter ξ as our representation of the phase space.

Finally let us review the squeezing properties of such states. Defining the quadrature operators of the field in the usual way

$$X_1 = \tfrac{1}{2}(a + a^\dagger), \quad X_2 = \frac{1}{2i}(a - a^\dagger) \tag{2.19}$$

where $[X_1, X_2] = i/2$, we obtain

$$\langle (\Delta X_1)^2 \rangle \langle (\Delta X_2)^2 \rangle \ge \tfrac{1}{16} . \tag{2.20}$$

Squeezing exists if either variance is less than $\frac{1}{4}$. For the SU(1,1) CS it is clear that $\langle X_i \rangle = 0$, $i = 1,2$, so that

$$\langle (\Delta X_{1,2})^2 \rangle = \langle K_0 \pm K_1 \rangle . \tag{2.21}$$

If $\phi = \pi$, we obtain, for $k = \frac{1}{4}$,

$$\langle (\Delta X_1)^2 \rangle = \tfrac{1}{4} e^{\theta}, \quad \langle (\Delta X_2)^2 \rangle = \tfrac{1}{4} e^{-\theta} . \tag{2.22}$$

Evidently, there is squeezing in X_2 along with enhanced fluctuations in X_1 for $\theta > 0$. This case corresponds to $\xi > 0$, i.e., a positive real number. We assume in what follows that all initial states are squeezed in this manner.

We now derive the classical map for the Hamiltonian of Eq. (2.7). It will be assumed that an initial SU(1,1) CS $|\xi_0\rangle$ (the $k = \frac{1}{4}$ is henceforth suppressed) is propagated without dispersion which is, of course, not true for the fully quantum-mechanical evolution. We first apply the pulse evolution operator U_p in Eq. (2.9) on $|\xi_0\rangle$. U_p, however, is a group transformation operator. Using the 2×2 non-Hermitian realization of the algebra,[25] its representation is found to be

$$U_{p(2\times 2)} = e^{-2i\gamma K_1}_{(2\times 2)} = \begin{pmatrix} \cosh\gamma & -i\sinh\gamma \\ i\sinh\gamma & \cosh\gamma \end{pmatrix} = \begin{pmatrix} \alpha & \beta \\ \beta^* & \alpha^* \end{pmatrix} . \tag{2.23}$$

Now for any group transformation operator $T(G)$ corresponding to the 2×2 group element

$$G = \begin{pmatrix} a & b \\ b^* & a^* \end{pmatrix}, \quad |a|^2 - |b|^2 = 1 , \tag{2.24}$$

the action of $T(G)$ on an SU(1,1) CS $|\xi'\rangle$ is

$$T(G)|\xi\rangle = e^{i\Phi}|\xi'\rangle \tag{2.25}$$

where

$$\xi' = R(\xi) = \frac{a\xi + b}{b^*\xi + a^*}, \quad \Phi = 2k \arg(a^* + b^*\xi) . \tag{2.26}$$

(The unimodular Möbius transformation R maps the unit circle $|\xi| = 1$ and its interior $|\xi| < 1$ one to one and onto

themselves, respectively.) Thus, for our case,

$$U_p|\xi_0\rangle = e^{i\Phi_0}|\xi_0'\rangle \tag{2.27}$$

where

$$\xi_0' = \frac{\cosh\gamma\xi_0 - i\sinh\gamma}{i\sinh\gamma\xi_0 + \cosh\gamma} \equiv -\tanh\left[\frac{\theta_0'}{2}\right]e^{-i\phi_0'} . \tag{2.28}$$

Apparently

$$\theta_0' = 2\tanh^{-1}(|\xi_0'|) \tag{2.29}$$

which will be needed for the "free" evolution part. The phase $\Phi_0 = 2k\arg(a^* + b^*\xi)$ is not used in what follows.

Between the pulses we simply solve the classical equations of motion for ξ, given by[26]

$$\dot{\xi} = \{\xi, \mathcal{H}\} , \tag{2.30}$$

where the Poisson bracket is

$$\{A,B\} = \frac{(1-|\xi|^2)^2}{2ik}\left[\frac{\partial A}{\partial\xi}\frac{\partial B}{\partial\xi^*} - \frac{\partial A}{\partial\xi^*}\frac{\partial B}{\partial\xi}\right] \tag{2.31}$$

and $\mathcal{H} = \langle \xi,k|H|\xi,k\rangle$. Between pulses $H_I = 2\lambda K_+ K_-$, and

$$\mathcal{H}_I = 2\lambda\langle K_+K_-\rangle \simeq 2\lambda\langle K_+\rangle\langle K_-\rangle \tag{2.32}$$

where the mean-field approximation[27] has been made. Using the fact that

$$\langle K_+\rangle = \langle K_-\rangle^* = \frac{-2k\xi^*}{(1-|\xi|^2)} = -k\sinh\theta e^{i\phi} \tag{2.33}$$

the equations of motion may be integrated over the interval from $t=0$ to $t=T$ to obtain

$$\xi(T) = \xi_0' e^{-i\Omega_0 T} \equiv \xi_1 , \tag{2.34}$$

where

$$\Omega_0 = 4\lambda k\cosh\theta_0' = \lambda\cosh\theta_0'$$

and θ_0' is determined from Eq. (2.29). $|\xi_1\rangle$ is then subjected to the next pulse, and so on, to obtain the stroboscopic map relating ξ_{n-1} to ξ_n:

$$\xi_n = \left[\frac{\cosh\gamma\xi_{n-1} - i\sinh\gamma}{i\sinh\gamma\xi_{n-1} + \cosh\gamma}\right]e^{-i\Omega_{n-1}T} , \tag{2.35}$$

where

$$\Omega_{n-1} = \lambda\cosh\theta_{n-1}' \tag{2.36}$$

and

$$\theta_{n-1}' = 2\tanh^{-1}\left[\left|\frac{\cosh\gamma\xi_{n-1} - i\sinh\gamma}{i\sinh\gamma\xi_{n-1} + \cosh\gamma}\right|\right] . \tag{2.37}$$

An alternate way of producing a classical map involves the use of the Heisenberg equations to obtain the evolution of the operators K_0 and $K_\pm$. Actually we use the Heisenberg equation between pulses and the operator U_p over the pulses. When $t \neq nT$ [hence $\delta_p(t) = 0$], Heisenberg's equation for K_- is

$$i\hbar\dot{K}_- = [K_-, H_I] = (4\lambda K_0)K_- = \Omega(K_0)K_- \tag{2.38}$$

where $\Omega(K_0) \equiv 4\lambda K_0$. The equation for K_0 is

$$i\hbar\dot{K}_0 = [K_0, H_I] = 0 , \tag{2.39}$$

which implies that K_0 is constant between pulses. The solution to Eq. (2.38) is therefore

$$K_-(t_2) = \exp[-i\Omega(K_0)(t_2 - t_1)]K_-(t_1) , \tag{2.40}$$

$$K_0(t_2) = K_0(t_1) . \tag{2.41}$$

Of course, from (2.40), it also follows that

$$K_+(t_2) = K_+(t_1)\exp[i\Omega(K_0)(t_2 - t_1)] . \tag{2.42}$$

Over the pulses the evolution of the operators K_i $(i = 0, \pm)$ is given by

$$\bar{K}_i = U_p^\dagger K_i U_p \tag{2.43}$$

where K_i denotes the operator just prior to pulsing, and $\bar{K}_i$ just after pulsing. With U_p given by Eq. (2.9) and with the use of Baker-Hausdorff formulas we obtain

$$\bar{K}_0 = e^{2i\gamma K_1}K_0 e^{-2i\gamma K_1}$$

$$= K_0\cosh(2\gamma) + \frac{1}{2i}(K_+ - K_-)\sinh(2\gamma) , \tag{2.44}$$

$$\bar{K}_+ = K_+\cosh^2(\gamma) - K_-\sinh^2(\gamma) + iK_0\sinh(2\gamma) , \tag{2.45}$$

$$\bar{K}_- = K_-\cosh^2(\gamma) - K_+\sinh^2(\gamma) - iK_0\sinh(2\gamma) . \tag{2.46}$$

If we denote the operators just prior to the nth pulse as $K_\pm(n)$ and $K_0(n)$, then just after the nth pulse, from Eqs. (2.44–2.46), they are given by

$$\bar{K}_+(n) = K_+(n)\cosh^2(\gamma) - K_-(n)\sinh^2(\gamma) + iK_0(n)\sinh(2\gamma) , \tag{2.47}$$

$$\bar{K}_-(n) = K_-(n)\cosh^2(\gamma) - K_i(n)\sinh^2(\gamma) - iK_0(n)\sinh(2\gamma) , \tag{2.48}$$

$$\bar{K}_0(n) = K_0(n)\cosh(2\gamma) + \frac{1}{2i}[K_+(n) - K_-(n)]\sinh(2\gamma) . \tag{2.49}$$

Over the "free" evolution time up to just before the $(n+1)$ pulse, from Eqs. (2.40)–(2.42),

$$K_+(n+1) = \bar{K}_+(n)\exp[i\Omega(\bar{K}_0(n))T] , \tag{2.50}$$

$$K_-(n+1) = \exp[-i\Omega(\bar{K}_0(n))T]\bar{K}_-(n) , \tag{2.51}$$

$$K_0(n+1) = \overline{K_O}(n) , \tag{2.52}$$

where $\Omega(\bar{K}_0(n)) = 4\lambda\bar{K}_0(n)$. Thus $K_0(n)$ and $K_\pm(n)$ are related to $K_0(n+1)$ and $K_\pm(n+1)$ by

$$K_+(n+1) = [K_+(n)\cosh^2(\gamma) - K_-(n)\sinh^2(\gamma) + iK_0(n)\sinh(2\gamma)]\exp[4i\gamma TK_0(n+1)] , \tag{2.53}$$

$$K_-(n+1)=\exp[-4i\lambda T K_0(n+1)] \times[K_-(n)\cosh^2(\gamma)-K_+(n)\sinh^2(\gamma) -iK_0(n)\sinh(2\gamma)] , \quad (2.54)$$

and

$$K_0(n+1)=K_0(n)\cosh(2\gamma) +\frac{1}{2i}[K_+(n)-K_-(n)]\sinh(2\gamma) . \quad (2.55)$$

These equations define the quantum maps for the operators K_0 and $K_\pm$.

To obtain classical maps, we define the scaled operators $X_\pm=K_\pm/k$, $X_0=K_0/k$. With the assumption of large k (the classical limit[27]), the commutators of these operators vanish, i.e.,

$$[X_+,X_-]=\frac{2}{k}X_0\to 0 , \quad (2.56)$$

$$[X_\pm,X_0]=\mp\frac{1}{k}X_\pm\to 0 \text{ as } k\to\infty . \quad (2.57)$$

The Casimir operator becomes

$$C=K_0^2-\tfrac{1}{2}(K_+K_-+K_-K_+)=k^2(X_0^2-X_+X_-) . \quad (2.58)$$

Since the eigenvalue of C is k^2 in the limit of large k, we deduce that

$$X_0^2-X_+X_-=1 , \quad (2.59)$$

which implies that the motion in X space is confined to a unit hyperboloid. In the classical limit of large k, the quantum map becomes

$$X_+(n+1)=\exp[4i\lambda T k X_0(n+1)] \times[X_+(n)\cosh^2(\gamma)-X_-(n)\sinh^2(\gamma) +iX_0(n)\sinh(2\gamma)] , \quad (2.60)$$

$$X_-(n+1)=X_+^*(n+1) , \quad (2.61)$$

$$X_0(n+1)=X_0(n)\cosh(2\gamma) +\frac{1}{2i}[X_+(n)-X_-(n)]\sinh(2\gamma) . \quad (2.62)$$

To get a picture of the map it is sufficient to project the motion only onto the X_1,X_2 plane where $X_\pm=X_1\pm iX_2$. The connection to the previous formulation of the map is easily made by setting $X_0=\cosh\theta$, $X_\pm=-\sinh\theta e^{\pm i\phi}$. Then

$$\theta=\cosh^{-1}(X_0) , \quad \phi=\tan^{-1}\left[\frac{1}{i}\left[\frac{X_+-X_-}{X_++X_-}\right]\right] . \quad (2.63)$$

Finally, we consider the full quantum-mechanical motion. First note that in the basis $|m,k\rangle$, the operators K_+ and K_- have the actions

$$K_+|m,k\rangle=[(m+1)(m+2k)]^{1/2}|m+1,k\rangle , \quad (2.64)$$

$$K_-|m,k\rangle=[m(m+2k-1)]^{1/2}|m-1,k\rangle . \quad (2.65)$$

Thus K_+K_- is diagonal in this basis,

$$K_+K_-|m,k\rangle=m(m+2k-1)|m,k\rangle . \quad (2.66)$$

Therefore the matrix elements of the evolution operator are

$$U_{mn}=\langle m,k|U|n,k\rangle=e^{-2i\lambda T[m(m+2k-1)]}\mathcal{V}^k_{m,n}(\alpha,\beta) \quad (2.67)$$

where

$$\mathcal{V}^k_{m,n}(\alpha,\beta)=\langle m,k|e^{-2i\gamma K_1}|n,k\rangle \quad (2.68)$$

is a Bargmann function for the finite SU(1,1) transformation given by Eq. (2.23). These functions may be evaluated in terms of hypergeometric functions as

$$\mathcal{V}^k_{m,n}(\alpha,\beta)=A_{nm}(\alpha^*)^{-m-n-2k}(-\beta^*)^{n-m} \times{}_2F_1(-m,1-m-2k,n-m+1;-\beta^*\beta) , \quad m\le n , \quad (2.69)$$

$$\mathcal{V}^k_{m,n}(\alpha,\beta)=A_{mn}(\alpha)^{m-n-2k}(\beta)^{m-n} \times{}_2F_1(-n,1-n-2k,1+m-n;-\beta^*\beta) , \quad m\ge n , \quad (2.70)$$

where

$$A_{mn}=\frac{1}{\Gamma(1+m-n)}\left[\frac{\Gamma(m+1)\Gamma(m+2k)}{\Gamma(n+1)\Gamma(n+2k)}\right]^{1/2} \quad (2.71)$$

and, from Eq. (2.23), $\alpha=\cosh\gamma$ and $\beta=-i\sinh\gamma$.

In closing this section we wish to mention that at first glance, it might seem that the method we have used to calculate the time evolution over the pulse is very cumbersome and that one might just as well diagonalize K_1 itself rather than the evolution operator. Such a procedure would be valid in the case of the kicked top where the generators of SU(2) always have discrete spectra and the Hilbert space is finite dimensional. However, for SU(1,1), the operator K_1 cannot be diagonalized within a $\mathcal{D}^+(k)$ representation. Rather, it has a continuous spectrum and in fact, physically corresponds to an inverted oscillator. In terms of x and p,

$$K_1=\tfrac{1}{4}(p^2-x^2) . \quad (2.72)$$

Because of this fact, there are significant differences between the present system under study and the problems of the kicked top. Further consequences of this will be discussed in the next section.

III. RESULTS

Before getting into the details of our results, we first discuss some of the technicalities of our numerical computations with particular regard to the truncation scheme employed. As already pointed out, for SU(1,1) as opposed to SU(2), the relevant Hilbert spaces are infinite dimensional and therefore an appropriate truncation scheme is required. In the $|m,k\rangle$ basis, in which K_0 is diagonal, the matrix elements of the unitary time evolu-

tion operator are known analytically and given by Eq. (2.67).

An accurate computation of the hypergeometric functions in Eqs. (2.69) and (2.70) represents one of the first difficult challenges encountered in the numerical work. Even though these functions reduce to polynomials (with terms alternating in sign), evaluation becomes difficult for $\gamma \gtrsim 1$ and $m \sim m' \gtrsim 70$. The individual terms in the sum become quite large for the diagonal elements and unavoidable roundoff errors may dominate. In order to estimate the error we have summed the terms in the polynomial in both directions and compared the results. As a further check, the polynomial was computed using the symbolic manipulation program MAPLE (Ref. 28) which supports floating point calculations to any specified number of digits. With these two checks we could control the accuracy of the individual matrix elements for $\gamma \lesssim 0.1$ and with matrix dimension $m_{\max}=200$.

We now discuss the structure of the spectrum of U. It is worthwhile to mention the special case of the evolution operator when $\lambda=0$ and the total dynamics is governed by the generator K_1. As stated earlier, K_1 corresponds to an inverted harmonic oscillator with no discrete spectrum. In this case, however, the classical and quantum evolutions agree and it can be shown[21] that the average photon number increases rapidly with increasing time. Consequently, the eigenmodes cannot be localized in a discrete Fock state basis. Therefore it is clear that any finite dimensional discrete basis approximation will fail for this special case. However, for $\lambda \neq 0$, the spectrum of U is discrete. This can easily be understood as follows: the terms K_+K_- correspond to an attractive nonlocal anharmonic oscillator containing terms like x^4. Clearly as $x \to \infty$, these anharmonic terms will dominate over the $-x^2$ of the inverted oscillator part. From a classical point of view, the motion in phase space is restricted and therefore we expect the spectrum to be discrete.

It is clear that the restriction to a finite number of basis vectors is only appropriate for approximating those eigenmodes which are appreciably excited by the initial state and essentially localized within the truncated basis. These localized eigenmodes can be easily identified via the modulus of their corresponding eigenvalues. The larger the overlap with the truncated discrete basis the closer the eigenvalue is to be found near the unit circle. For example, for $\gamma=0.05$, $\lambda T=5$, and 200 basis states, 75% of the eigenvalues have modulus in the range [0.99, 1.0]. As an additional check the number of basis states was doubled. Those eigenvalues with unit modulus near the unit circle remained unchanged whereas the others changed significantly.

Excited nonlocalized modes would lead to an artificial damping in our model, which was carefully monitored by checking the normalization of the state vector after each iteration. For an initial state $|\xi,k\rangle$ with $k=\frac{1}{4}$ and $|\xi| \leq 0.9$, the norm remained constant at unity to within one part in 10^5.

As an independent check of our truncation, the expectation value of the Casimir operator C [Eq. (2.12)] was computed as a function of time. Recall that C is a constant of motion for our system, with $k=\frac{1}{4}$, $\langle C \rangle = -\frac{3}{16}$. This value was obtained by retaining only the first 200 basis vectors for $|\xi| \leq 0.9$ in the initial state.

Having discussed the computational technicalities we now present the results, first focusing on the classical map given by Eqs. (2.35)–(2.37). At first sight, this map may be considered as a composition of a nonlinear rotation about the origin in the ξ plane and a unimodular Möbius transformation with constant coefficients. The rotation is nonlinear because the angle $\Omega_{n-1}T$ depends on $|\xi_{n-1}|$. (This transformation produces a shear in an ensemble of initial points with differing $|\xi|$ values. Repeated application would distribute the iterates over concentric circles.) However, the ξ map in Eq. (2.35) is itself a Möbius transformation of the form in Eq. (2.26) with time- (n) dependent coefficients, viz.,

$$\xi_n = R_n(\xi_{n-1}) = \frac{a_{n-1}\xi_{n-1}+b_{n-1}}{b_{n-1}^*\xi_{n-1}+a_{n-1}^*} , \tag{3.1}$$

where

$$a_{n-1} = e^{-i\Omega_{n-1}T/2}\cosh\gamma ,$$
$$b_{n-1} = -ie^{-i\Omega_{n-1}T/2}\sinh\gamma . \tag{3.2}$$

Möbius transformations were encountered in Ref. 21. Note that in this case, when no anharmonicity is present, i.e., $\lambda=0$, then the transformations become time-independent, i.e., $a_n=a, b_n=b$, and the dynamics becomes quite simple (see Ref. 21, Sec. III). The unimodular Möbius transformations are one-to-one maps of the phase space, the Lobachevski plane $|\xi|<1$, onto itself. They are area preserving (our system is Hamiltonian) in the proper metric: the invariant measure is[17]

$$\frac{2k-1}{\pi}\frac{d^2\xi}{(1-|\xi|^2)^2} , \tag{3.3}$$

which accounts for the term appearing in the Poisson brackets of Eq. (2.31). In order to understand the dynamics in the Lobachevski plane from a geometrical viewpoint, consider the mapping for the classical quantities X_i in Eqs. (2.60)–(2.62). From Eq. (2.59), the variables X_0, X_1, and X_2 are constrained to move on a hyperboloid. The relations in Eq. (2.63) effectively project this motion onto the interior of the unit circle of the ξ plane. In the case $\lambda=0$, i.e., no anharmonicity, the Möbius transformation may have a fixed point on the unit circle $|\xi|=1$. On the hyperboloid, however, this fixed point corresponds to infinity, and the values of X_0, X_+, and X_- increase toward infinity with the restriction of Eq. (2.59). The approach to a fixed point observed in the ξ plane is thus seen to be an artifact of the geometry involved in the projection. [The unimodular Möbius transformations form a group of *hyperbolic rotations* which map both halves of the cones

$$X_0^2 - X_1^2 - X_2^2 = \text{const} > 0 \tag{3.4}$$

onto themselves. These cones are subspaces of a pseudo-Euclidean space of signature (1,2). In our case, the constant is 1. These rotations leave invariant the Euclidean measure $d\mathbf{X}=dX_0dX_1dX_2$.]

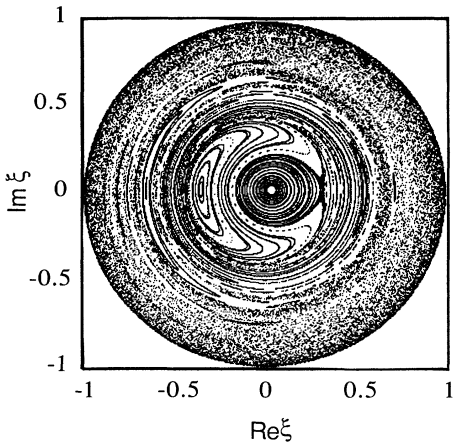

FIG. 1. Classical map for $\gamma=0.05$, $\lambda T=5$. One hundred different initial points along the real axis have been chosen and each point has been iterated 1200 times.

In Fig. 1, we plot the first 1200 iterations of the classical map for 100 different initial conditions taken along the real line in the ξ plane, with $\gamma=0.05$ and $\lambda T=5$. A mixture of regular and irregular motion is observed in phase space. For an initial ξ value close to the origin ($|\xi| \lesssim 0.2$), all iterates stay on a circle whose center corresponds to a fixed point of the map. For $|\xi| \gtrsim 0.6$ the iterates almost uniformly fill up a broad circular strip. With increasing λT and γ, the size of the domains of regular motion decreases.

We now turn to the quantum-mechanical manifestations of the regular and chaotic classical motions. The following discussion is restricted to the case where the corresponding classical motion is given in Fig. 1. That is, we shall compare the quantum dynamics of states initially centered in either the regular or chaotic regions of the corresponding classical motion.

As a first comparison we consider the dephasing of an initial SU(1,1) CS. If the initial state ($n=0$) is $|\psi(n=0)\rangle=|\xi,k\rangle$, then after n pulses the state is

$$|\psi(n)\rangle=U^n|\psi(0)\rangle \ . \tag{3.5}$$

The initial-state population probability is defined as

$$P(n)=|\langle\psi(0)|\psi(n)\rangle|^2 \ . \tag{3.6}$$

This notion has previously been used in the comparison of the quantum dynamics for Gaussian wave packets initially centered in regions of regular or chaotic motion in phase space for systems such as the Hénon-Heiles Hamiltonian.[29] There it was found that for wave packets initially centered in regular regions the initial-state population probability showed regular quasiperiodic revivals whereas for a wave packet centered in a chaotic region, a rapid dephasing was observed. This dephasing of the initial-state population probability is only one of the proposed signals of quantum chaos. In our case the initial wave packets are "squeezed" Gaussians.[30] In Fig. 2 is plotted $P(n)$ versus n for two initial SU(1,1) CS's, one

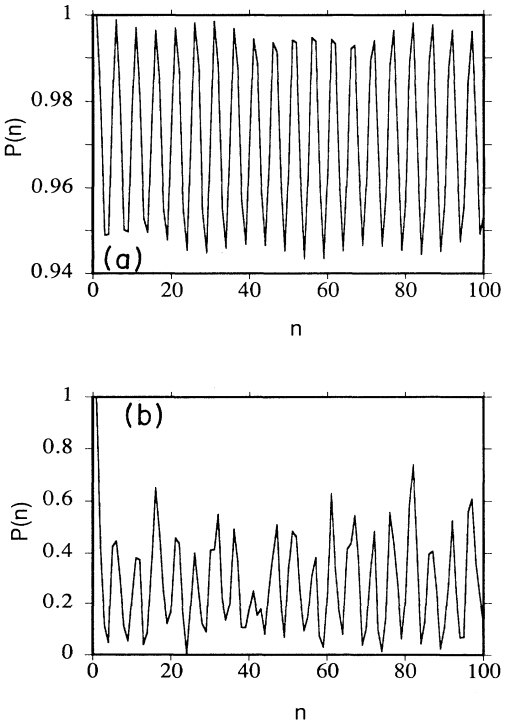

FIG. 2. Initial-state population probability $P(n)$ vs time n for (a) $|\xi|=0.2$ and (b) $|\xi|=0.9$.

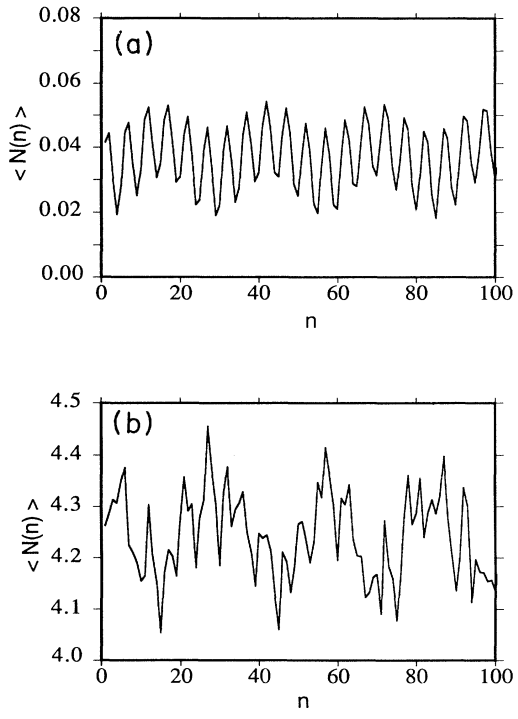

FIG. 3. Average photon number $\langle N(n)\rangle$ vs time n for (a) $|\xi|=0.2$ and (b) $|\xi|=0.9$.

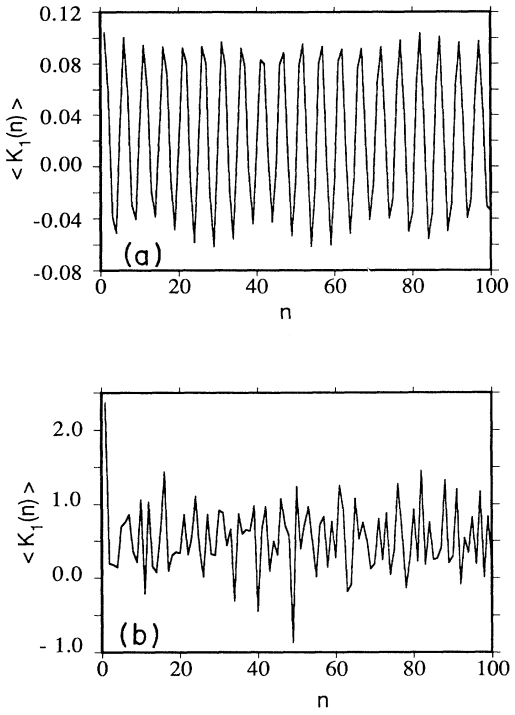

FIG. 4. Expectation value of K_1 vs time n for (a) $|\xi|=0.2$ and (b) $|\xi|=0.9$.

chosen from the regular region ($|\xi|=0.2$) and the other from the chaotic region ($|\xi|=0.9$). It is quite clear from the figure that the quantum evolutions are qualitatively different in each case. In the regular case, essentially only two eigenmodes of the unitary propagator are excited and carry most of the weight of the initial state. The overlap varies only slightly from its initial value and we observe regular and complete revivals of $P(n)$. In the chaotic case, a few more modes are excited and $P(n)$ rapidly dephases almost to zero within one time step. However, since only a small number of available eigenmodes were significantly excited the overlap does not stay at the minimum value but rather oscillates erratically. We speculate that for higher values of γ, more eigenmodes would be excited and that $P(n)$ would be essentially zero for $n>0$. However, as explained, high values of γ are not accessible in our numerical calculations.

In Fig. 3 is plotted the mean photon number $\langle N(n)\rangle$ as a function of time (n). For very low initial photon number (regular regime) the oscillations in $\langle N(n)\rangle$ are small and essentially quasiperiodic. Actually the presence of two frequencies is evident in Fig. 3(a). However, for larger initial photon number (chaotic regime) the fluctuations in $\langle N(n)\rangle$ are considerably greater, as seen in Fig. 3(b), and the motion is quite erratic. Nevertheless, the number of frequencies is apparently still quite small which corresponds, as stated earlier, to the fact that few eigenmodes of the U operator are excited for the chosen values of γ and λT. It appears that quantum mechanics greatly suppresses the classical chaotic motion in this model. In Fig. 4 we see that the expectation value of the

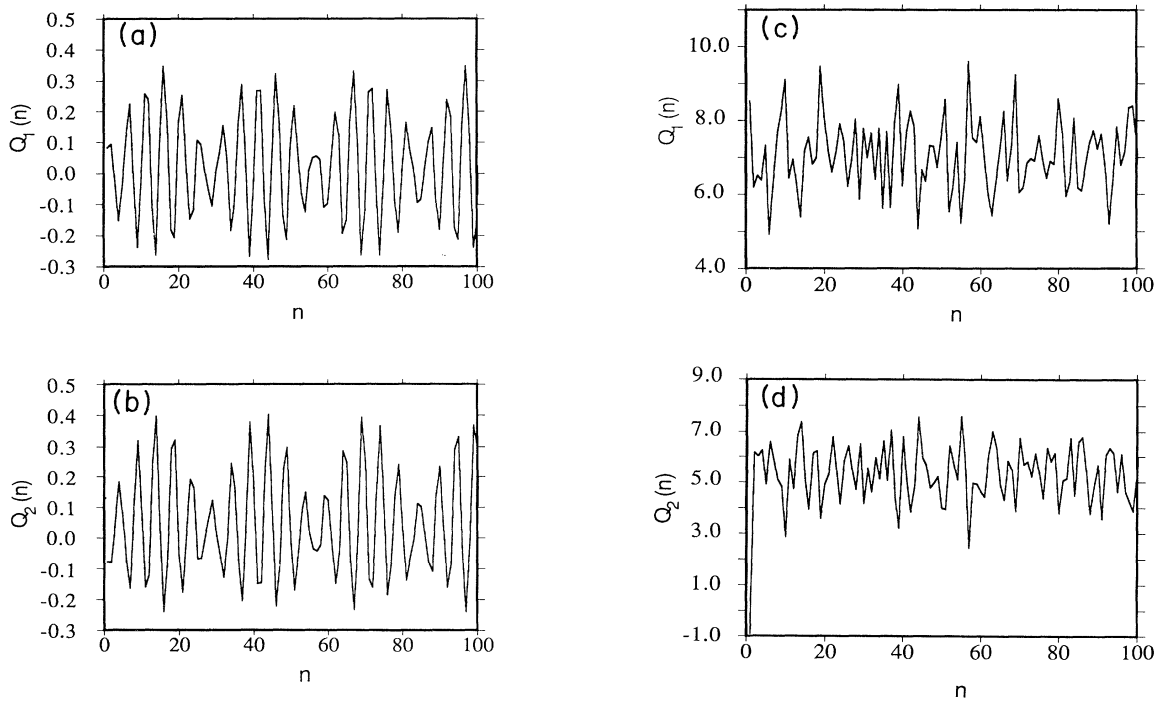

FIG. 5. (a) Q_1 vs time n for $|\xi|=0.2$. (b) Q_2 vs time n for $|\xi|=0.2$. (c) Q_1 vs time n for $|\xi|=0.9$. (d) Q_2 vs time n for $|\xi|=0.9$.

operator K_1 displays behavior in time similar to that of N (or K_0).

Since our initial states are taken to be squeezed states (actually squeezed vacuum states), it is worthwhile to study the time evolution of the squeezing property. In order to characterize the squeezing it is convenient to define the parameters[31]

$$Q_{1,2}=\frac{\langle(\Delta X_{1,2})^2\rangle-0.25}{0.25} \tag{3.7}$$

where $\langle(\Delta X_{1,2})^2\rangle$ are given by Eqs. (2.21). For $Q_{1,2}$ in the range $-1\leq Q_{1,2}<0$ squeezing exists. When ξ is initially real, squeezing occurs in the X_2 quadrature. In Fig. 5 are plotted Q_1 and Q_2 for $|\xi|=0.2$. Note that the initial squeezing is revoked from X_2, accompanied by simultaneous squeezing in X_1. The oscillations in the Q_i are essentially quasiperiodic with two evident frequencies. However, for $|\xi|=0.9$, X_2 is initially highly squeezed but the squeezing is revoked immediately after the first kick and does not recur. Also no squeezing develops in the X_1 quadrature.

In the preceding quantum-mechanical calculations, the time evolution has been characterized by the excitation of only a very few eigenmodes of U by the initial SU(1,1) CS. This feature was unchanged when the initial state was taken to be a number state $|m,k=\frac{1}{4}\rangle$ with $2\leq m\leq 50$. As a further test for localized eigenmodes we have analyzed the fluctuation properties of the quasienergies ϕ_n of the propagator U defined as

$$U|\Phi_n\rangle=e^{i\phi_n}|\Phi_n\rangle \tag{3.8}$$

where $|\Phi_n\rangle$ denote the eigenvectors of U. The fluctuations of the nearest-neighbor quasienergy spacings $s_n=\phi_{n+1}-\phi_n$ can be conveniently analyzed via the so-called level statistics distribution function $P(s)$. $P(s)ds$ denotes the probability of finding the nearest-neighbor eigenvalue in the interval $[s,s+ds]$. The quasienergy level statistics has been established as a rather reliable tool to evaluate the degree of localization of the eigenvectors $|\Phi_n\rangle$ in their natural basis representation.[32] The localization of eigenvectors is quite common in classically regular systems (for example, the kicked spinning top[5]) and in some models also in the chaotic regime (e.g., the kicked rotator[32]). For our model, which is invariant under time reversal,[32] we would expect a spacing distribution approximately described by the Wigner function

$$P(s)=\frac{\pi}{4}se^{(-\pi/2)s^2} \tag{3.9}$$

if the eigenmodes were delocalized and had an appreciable overlap with all the states in the $|m,k\rangle$ basis. In Fig. 6 is plotted the calculated distribution of nearest-neighbor quasienergies for our evolution operator U. For comparison we have also plotted the Wigner and Poisson $[P(s)=e^{-s}]$ distributions. As expected we find numerically the Poisson distribution which corresponds to the localization of the eigenmodes $|\Phi_n\rangle$. In order to obtain more reliable statistics we have discarded those few eigenvalues whose moduli are not close to unity and found the distribution essentially unchanged. At this stage we cannot exclude the possibility that the eigenmodes extend further with increasing parameters γ or λT. By comparison, the eigenmodes of the kicked rotator become more extended with increasing perturbation.[33]

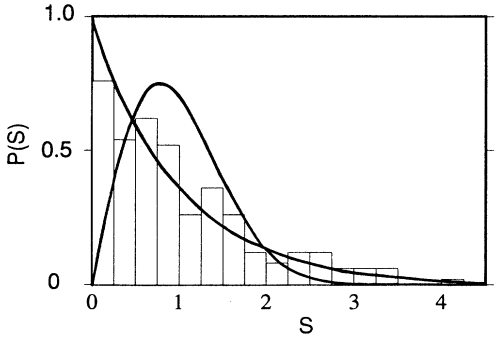

FIG. 6. The nearest-neighbor quasi-energy spacing histogram for the evolution operator U with $\lambda T=5$, $\gamma=0.05$, and 200 basis states retained. The two curves correspond to Poisson and Wigner distributions.

IV. CONCLUSION

In summary we have presented a nonlinear quantum-optical model whose classical counterpart can exhibit chaotic as well as regular motion. The quantum signatures of the classically regular and chaotic motion in the initial-state population probability and in the time-dependent expectation values are similar to those seen in other quantum chaotic models although it must be said that for the chaotic case, the signatures are not as distinct here. On the other hand, it should be noted that it is quite possible to produce some of these signatures of quantum chaos even in models where there is not even classically chaotic motion.[21,23,34,35] We might expect the quantum chaotic behavior of our SU(1,1) system to become more apparent in the limit that the Bargmann index k becomes large. This limit has previously been shown to be the classical limit of SU(1,1) Hamiltonian systems.[27,36] We stress, however, that only the values $k=\frac{1}{4}$ (squeezed vacuum states) or $k=\frac{3}{4}$ (squeezed one-photon states) are physically relevant to quantum optics. Nevertheless, this point is worth investigating and we hope to discuss it elsewhere.

A paper by Milburn[37] has recently appeared in which a system similar to the one studied here was examined. However, the initial states were taken to be ordinary coherent states. Our paper may be considered as complementary to Ref. 37.

ACKNOWLEDGMENTS

C.C.G. thanks the Graduate School of St. Bonaventure University for a grant in aid of research. He also acknowledges the hospitality of the quantum optics group at the University of Rochester where this work was completed. R.G. acknowledges support by the Alexander von Humboldt Foundation of West Germany. E.R.V. gratefully acknowledges a grant in aid of research from the Natural Sciences and Engineering Research Council of Canada.

[1]See, for example, the review by B. Eckhardt, Phys. Rep. **163**, 205 (1988).
[2]G. M. Zaslavsky, Phys. Rep. **80**, 157 (1981).
[3]G. Casati, B. V. Chirikov, J. Ford, and F. M. Izrailev, in *Stochastic Behavior in Classical and Quantum Hamiltonian Systems,* edited by G. Casati and J. Ford (Springer, Berlin, 1979).
[4]S. -J. Chang and K. -J. Shi, Phys. Rev. A **34**, 7 (1986).
[5]F. Haake, M. Kuś, and R. Scharf, Z. Phys. B **65**, 381 (1987); R. Grobe and F. Haake, *ibid.* **68**, 503 (1987).
[6]See the review by R. Loudon and P. L. Knight, J. Mod. Opt. **34**, 709 (1987).
[7]K. Życzkowski, J. Phys. A **22**, L1147 (1989).
[8]R. E. Slusher, L. W. Hollberg, B. Yurke, J. C. Mertz, and J. F. Valley, Phys. Rev. Lett. **55**, 2409 (1985); R. M. Sheley, M. D. Levenson, S. H. Perlmutter, R. G. Devoe, and D. F. Walls, *ibid.* **57**, 691 (1986); L. -A. Wu, H. J. Kimble, J. L. Hall, and H. Wu, *ibid.* **57**, 520 (1986).
[9]P. D. Drummond and D. F. Walls, J. Phys. A **13**, 725 (1980).
[10]P. Tombesi and H. P. Yuen, in *Coherence and Quantum Optics V,* edited by L. Mandel and E. Wolf (Plenum, New York, 1984), p. 751.
[11]C. C. Gerry and S. Rodriguez, Phys. Rev. A **36**, 5444 (1987).
[12]C. C. Gerry and E. R. Vrscay, Phys. Rev. A **37**, 4265 (1988).
[13]K. Wódkiewicz and J. H. Eberly, J. Opt. Soc. Am. B **2**, 458 (1985).
[14]C. C. Gerry, Phys. Rev. A **31**, 2721 (1985).
[15]C. C. Gerry, Phys. Rev. A **35**, 2146 (1987).
[16]A. M. Perelomov, Commun. Math. Phys. **26**, 222 (1972).
[17]A. Perelomov, *Generalized Coherent States and Their Applications* (Springer, Berlin, 1986).
[18]A. Inomata, S. Kuratsuji, and C. C. Gerry (unpublished).
[19]C. C. Gerry, Phys. Rev. A **37**, 2638 (1988).
[20]C. C. Gerry and C. Johnson, Phys. Rev. A **40**, 278 (1989).
[21]C. C. Gerry and E. R. Vrscay, Phys. Rev. A **39**, 5717 (1989).
[22]Y. Pomeau, B. Dorizzi, and B. Grammaticos, Phys. Rev. Lett. **56**, 681 (1986).
[23]P. W. Milonni, J. R. Ackerhalt, and M. E. Goggin, Phys. Rev. A **35**, 681 (1987).
[24]See P. K. Aravind, J. Opt. Soc. Am. B **5**, 1545 (1988).
[25]See, for example, B. G. Wyboure, *Classical Groups for Physicists* (Wiley, New York, 1974), Chap. 17 and references therein. See also Refs. 17 and 18.
[26]C. C. Gerry and S. Silverman, J. Math. Phys. **23**, 1995 (1982); C. C. Gerry, Phys. Lett. **142B**, 391 (1984).
[27]C. C. Gerry, J. B. Togeas, and S. Silverman, Phys. Rev. D **28**, 1939 (1983).
[28]B. W. Char, K. O. Geddes, G. H. Gonnet, and S. M. Watt, *Maple User's Guide* (WATCOM, Waterloo, 1985).
[29]Y. Weissman and J. Jortner, Phys. Lett. **83A**, 55 (1981).
[30]See K. Wódkiewicz, J. Mod. Opt. **34**, 941 (1987).
[31]See C. K. Hong and L. Mandel, Phys. Rev. A **32**, 974 (1985).
[32]M. Feingold, S. Fishman, D. R. Grempel, and R. E. Prange, Phys. Rev. B **31**, 6852 (1985), and references therein.
[33]See, for example, M. Kus, R. Scharf, and F. Haake, Z. Phys. B **66**, 129 (1987), and references therein.
[34]C. C. Gerry, Phys. Lett. A (to be published).
[35]C. C. Gerry and T. Schneider, Phys. Rev. A **42**, 1033 (1990).
[36]C. C. Gerry and J. Kiefer (unpublished).
[37]G. J. Milburn, Phys. Rev. A **41**, 6567 (1990).